BEAM AND SPIN DYNAMICS IN AN ELECTRIC PROTON EDM RING

Richard Talman, Laboratory of Elementary Particle Physics,
Cornell University, Ithaca, NY 14850, USA
John Talman, Brookhaven National Laboratory, Upton, NY, 11973, USA

Abstract

Electric dipole moment (EDM) measurements may help to answer the question "Why is there more matter than antimatter in the present universe?" For a charged baryon like the proton such a measurement is thinkable only in a ring in which a bunch of protons is stored for more than a few minutes, with polarization "frozen" (relative to the beam velocity) and with polarization not attenuated by decoherence. Beam and spin dynamics in an all-electric lattice with these characteristics is described. Rings for other charged baryons, such as deuterons or helium-3 nuclei, are also possible but, requiring both electric and magnetic fields, they are more complicated.[1]

THEORETICAL MOTIVATION

The fundamental significance of electric dipole moments of fundamental particles has been understood for half a century, leading to experiments by Ramsay and others and theoretical speculations by Sakarov and others.

A 1981 paper by Ellis et al.[1] stated: "We argue that in a wide class of grand unified theories diagrams similar to those generating baryon number in the early universe also contribute to renormalization of the CP-violating θ parameter of QCD and hence to the neutron electric dipole moment d_n. We then deduce an order-of-magnitude lower bound on the neutron electric dipole moment: $d_n \approx 3\times10^{-28}$ e cm."

In a 1992 conference summary, Weinberg[2] stated: "Also endemic in supersymmetry theories are CP violations that go beyond the CKM matrix, and for this reason it may be that the next exciting thing to come along will be the discovery of a neutron or atomic or electron electric dipole moments. These electric dipole measurements seem to me to offer one of the most exciting possibilities for progress in particle physics. "

The 2007 Nuclear Science Advisory Committee (NSAC) Long Range Plan emphasized the importance of electric dipole moment (EDM) measurements for answering the question "Why is there more matter than antimatter in the present universe?". Until that time it was the neutron that seemed to be the most promising candidate for this measurement. It has recently been realized[3] that, stored for many minutes in a storage ring, the EDM's of proton, deuteron, and helium-3 nuclei may be measurable to better precision than can the neutron's.

Quite recently, introducing the 2011 Conference on Fundamental Physics at the Intensity Frontier, Arkani-Hamed[4] identified EDM's (along with quark and lepton flavor physics) as the areas of greatest promise.

[1] Partial support: the U.S. DOE, OSP Number: 62355/A001.

This paper discusses experimental practicalities of measuring the proton EDM. Methods for deuterons and ^{3}He nuclei will be similar.

SYMMETRY VIOLATIONS FOR A PARTICLE WITH BOTH MDM AND EDM

A magnetic dipole (MD) can be visualized as a loop of current lying in a plane; its axis is a pseudo-vector normal to the plane. An electric dipole (ED) can be visualized as separated charges (with vector pointing from positive to negative charge). Both types of vector can define the same plane, but they contain different geometric information. The magnetic pseudo-vector determines an in-plane rotational sense, but does not distinguish between the two sides of the plane. The electric vector does the opposite.

The ED and MD of the same particle cannot be said to be "parallel" without violating parity P—viewed in a mirror ED and MD would be anti-parallel. For ED and MD to be "parallel" would also violate time reversal T—run backwards, MD would reverse, ED would not.

Without any doubt, a proton has an MDM. For the proton to also have an EDM would imply the violation of both P and T symmetries. With CPT symmetry assumed, this would also implies the violation of CP symmetry. Violation of CP is a necessary condition for the cosmic evolution from balanced to unbalanced fractions of matter and anti-matter.

EDM-INDUCED SPIN PRECESSION

Numerically, in SI units, we can define $10^{-29}\,e$-cm to be a "nominal" EDM, $d_{\rm nom} = 10^{-29}\cdot(1.602\times10^{-19})\cdot(0.01) = (1.602\times10^{-50})$ [SI]. At our most optimistic, an EDM of this magnitude can be persuasively distinguished from zero in one year of running.

The ratio to nuclear magneton is $d_{\rm nom}/\mu_B = (1.602\times10^{-50})/(5.05\times10^{-27}) = 3.127\times10^{-24}$, with both numerator and denominator in SI units. This ratio is not dimensionless and cannot therefore be used to estimate the relative strength of electric and magnetic precession. The missing factor is E/B. For our configurations, in SI units, this ratio is typically $10^7/0.1\approx10^8$. After multiplying by this factor, the relative-effectiveness ratio *is* dimensionless and has a numerical value of about 3×10^{-16}. This is the approximate factor by which the EDM-induced precession is smaller than the (orthogonal) MDM-induced precession.

The rate of magnetic precession itself is large. For a pure Dirac particle in a magnetic field the precession is 2π per turn. At one microsecond per turn, this is of order 10^7 radians/s. Applying the E/B factor mentioned above, we therefore plan to measure a "nominal" EDM-induced

ISBN 978-3-95450-115-1

precession of order 10^{-9} r/s. After 10^5 s this would be 0.1 mr.

ALL-ELECTRIC STORAGE RING DESIGN

An all-electric storage ring is shown schematically in Fig. 1, and one cell of the lattice is shown in Fig. 2. Horizontal and vertical β-functions are shown in Fig. 3.

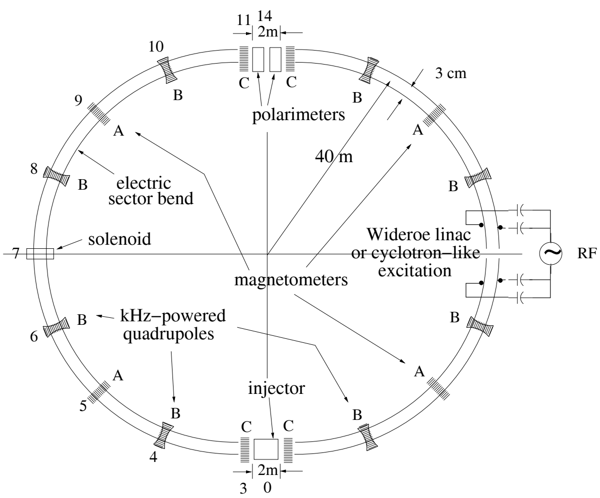

Figure 1: A very weak focusing all-electric lattice for measuring the electric dipole moment of the proton. Electric quadrupoles at the B locations tune the central vertical tune to, for example, $Q_{y,0} = 0.15$. Superimposed on this, one or more of the B quadrupoles "wobble" Q_y away from this value. By synchronous detection of the vertical separation of counter-circulating beams any radial magnetic field can be detected and nulled. With all electric bending, counter-circulating beams superimpose exactly, and all optical properties are identical for the two beams.

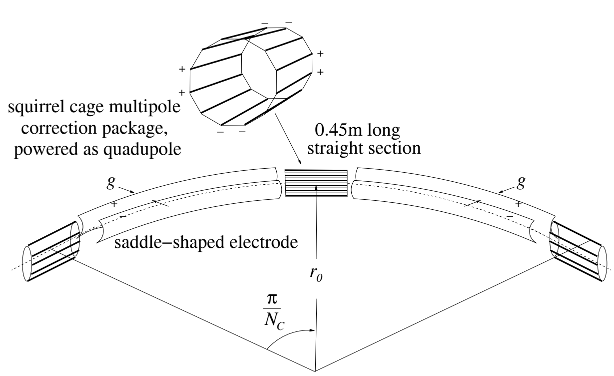

Figure 2: One cell of all-electric proton EDM lattice, with electrodes shaped for design field index m.

ESSENTIAL EXPERIMENTAL FEATURES

Design of this storage ring is dictated almost uniquely by the requirements of the experiment. Ideally the lattice would be purely weak focusing, with vertical tune

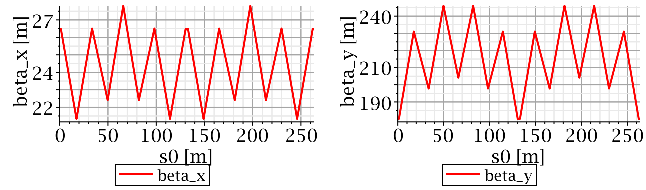

Figure 3: Plots of β functions of proton EDM lattice. β_y is *necessarily* very large, since Q_y has to be small.

$Q_y < 0.1$, with no straight sections, and with field index (defined below) $m \approx 0$. Accelerator practicalities force these requirements to be relaxed.

About 10^{10} protons need to be stored in multiple, low emittance, low energy spread, highly polarized bunches, for at least a quarter of an hour and preferably a day. The accumulated EDM effect is proportional to the run duration, and the statistical precision with which the polarization can be measured is limited by the number of protons available for the measurement. This requires high efficiency, polarization-preserving injection and storage.

The EDM signal is proportional to radial electric field E_r, which must therefore be maximized. We expect to achieve E_r=10 MV/m, leading to r_0=40 m. As shown in Fig. 4, there is a "magic" velocity β=0.6 for which the spin can be "frozen", parallel or anti-parallel to the proton velocity. Any EDM-induced spin precession will then accumulate monotonically. Stabilizing this configuration requires closed loop feedback from polarimeter to RF frequency. This is possible because the analyzing power of the proton carbon scattering used by the polarimeter exceeds 1/2 at the magic velocity. To reduce polarimeter bias the polarizations of circulating bunches alternate, forward and back.

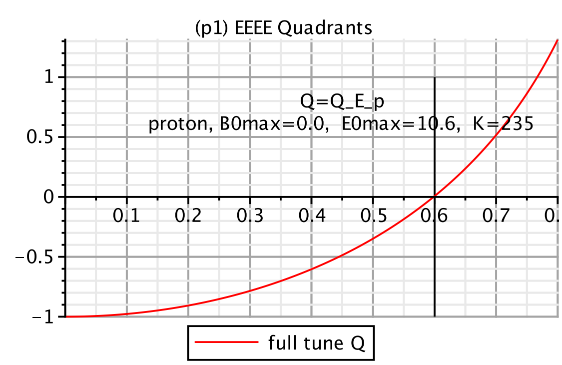

Figure 4: β-dependence of (magnetic) spin tune Q for protons in all-electric lattice. The spin is "globally frozen" for β=0.6. The spin is locally, but not globally, frozen for β=0.76, where Q is an integer other than zero.

Because, radial magnetic field acting on the magnetic moment mimics the EDM signal, several orders of magnitude suppression of magnetic field using both passive magnetic shielding and active B_r correction coil will be pro-

ISBN 978-3-95450-115-1

vided. Furthermore, current-matched counter-circulating beams will be stored, and the *difference* of their vertical polarizations measured. EDM-induced precessions will sum in this difference, while MDM-induced precessions cancel.

Counter-circulating beams provide another protection against MDM precession caused by radial magnetic field B_r. Any average radial magnetic field will produce vertical separation between the counter-circulating beams. Feeding back from vertical beam position (BPM) monitors to B_r compensation coils to null the vertical beam separation will force the average value of B_r to zero.

Squid magnetometers will be used for this nulling. Their precision is likely to dominate the systematic error of the measurement. In controlled lab environments squid magnetometers have been shown to provide the needed accuracy, but here they have to function in a (noisy) accelerator environment.

To improve the precision of vertical beam separation determination the vertical beam focusing will be made as weak as possible; for example the vertical tune will be as small as $Q_y = 0.1$.

Furthermore, by changing the strengths of one or more of the quadrupoles labelled B in Fig. 1, Q_y will oscillate about its nominal value, parametrically pumping the beam separation at a frequency in the kilohertz range, for which noise is minimal. Synchronous, lock-in detection of the vertical beam separation will permit greater BPM accuracy than is possible at existing storage rings.

Run duration may be determined by spin coherence time (SCT). One way of maximizing SCT is to reduce beam emittances. This can be done using electon cooling before data collection begins but, to avoid spurious spin precession, not during runs. Stochastic beam cooling may be possible throughout the runs.

"EXACT" UAL/ETEAPOT TRACKING

Most accelerator modeling programs assume that magnetic bending is dominant. For simulating the performance of an electric ring we need to account for the potential energy variation accompanying transverse position oscillations, an effect absent in magnetic elements. Within the Unified Accelerator Library (UAL) modeling framework[5] we have developed a code, ETEAPOT, patterned after TEAPOT[6], capable of simulating an all-electric ring.

An electric field with "field index" m power law dependence on radius r for y=0 is

$$\mathbf{E}(r,0) = -E_0 \frac{r_0^{1+m}}{r^{1+m}} \hat{\mathbf{r}}, \qquad (1)$$

and the electric potential $V(r)$, adjusted to vanish at $r = r_0$, is

$$V(r) = -\frac{E_0 r_0}{m}\left(\frac{r_0^m}{r^m} - 1\right). \qquad (2)$$

The "cleanest" case has m=1, which is the well-known Kepler or hydrogen atom case, except we must use relativistic mechanics. The Lorentz force equation is

$$\frac{d\mathbf{p}}{dt} = -k\,\frac{\hat{\mathbf{r}}}{r^2}, \qquad (3)$$

where k is the customary MKS notation for $1/(4\pi\epsilon_0)$ except for implicitly containing also a charge factor.

Remarkably, the exact 2D relativistic solution can be expressed in closed form for arbitrary amplitude[7][8][9]. The Muñoz/Pavic formulation[7], though consistent with other formalisms describing relativistic inverse square law orbits, is especially appropriate for our relativistic accelerator application. Their "generalized"-Hamilton vector

$$\mathbf{h} = h_r\,\hat{\mathbf{r}} + h_\theta\,\hat{\boldsymbol{\theta}} \qquad (4)$$

is especially convenient for describing 2D, relativistic accelerator orbits. Our 3D application can be formulated in such a way as to use only such 2D orbits. Though $\mathbf{h}$ is not conserved in general, it *is* conserved if and only if the orbit is circular, as it is on the central orbit of our proton EDM lattice. Neglecting the effects of the very weak, vertically focusing quads, off-momentum closed design orbits are also circles.

For long term tracking, we use this exact (and hence symplectic) m=1 evolution. But the actual storage ring field index value will have $m \neq 1$. To compensate for this incorrect focusing effect we "kick correct" to the actual m value, a process which also preserves symplecticity. In contrast to "approximate tracking in an exact lattice" this is "exact tracking in an approximate lattice"; this becomes fully accurate only in the limit of fine slicing.

The total energy,

$$\mathcal{E} = eV(\mathbf{r}) + \gamma(\mathbf{r}) m_p c^2, \qquad (5)$$

(rather than just the second term), is conserved (except for tiny changes passing through RF cavities.) So we recalculate $\gamma(\mathbf{r})$ whenever it is needed (e.g. to use Lorentz force to obtain the acceleration.) The angular momentum is

$$\mathbf{L} = \mathbf{r} \times \mathbf{p}. \qquad (6)$$

Both $\mathcal{E}$ and $\mathbf{L}$ are constants of the motion, but β and γ are not. This causes the conventional Courant-Snyder formalism to break down within electric elements, especially if the ring Twiss functions are required to be continuous. But the standard formalism can be consistently maintained *outside electric elements,* and then interpolated through them.

In terms of laboratory angle θ, the equations of motion reduce to

$$\boxed{\begin{aligned} \frac{dh_r}{d\theta} &= h_\theta, \\ \frac{dh_\theta}{d\theta} &= -\kappa^2\, h_r, \end{aligned}} \qquad (7)$$

where

$$\kappa^2 = 1 - \left(\frac{k}{Lc}\right)^2. \qquad (8)$$

These are the equations that justify having introduced the generalized Hamilton vector. Their general solution, valid at all amplitudes, can be written as

$$h_\theta = \mathcal{C}\,\cos\kappa(\theta-\theta_0)$$
$$h_r = \frac{\mathcal{C}}{\kappa}\,\sin\kappa(\theta-\theta_0). \qquad (9)$$

where θ is a running angle in the interior of the bend and θ_0 is an angle to be determined, along with $\mathcal{C}$, by matching to the known initial conditions.

For transverse orbit description, we replace Courant-Snyder 4D phase space description by the wobbling plane description illustrated in Fig. 5. The angular momentum pair (L_x, L_z), normal to the bend plane, rather than the pair (y, y') are evolved; re-scaled appropriately their numerical values can be adjusted to be the same to linear order.

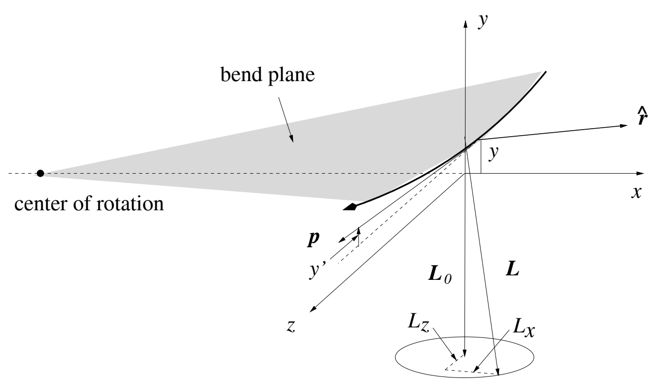

Figure 5: Wobbling-plane orbit coordinate definitions.

Our ETEAPOT evolution formalism has been checked against a conventional linearized transfer matrix formalism described, for example, by Wollnik[10]. Designed to be valid for all amplitudes, ETEAPOT tracking should certainly be accurate for the very small amplitudes for which the linearized formalism is valid. By tracking a bunch of standard particles having tiny, but non-zero, amplitudes, it is possible to extract approximate linear transfer matrix elements (by numerical differentiation). Tunes and β-functions can be obtained from these transfer matrices. Results of one such comparison are given in Table 1. The agreement is excellent. To the extent there is disagreement it is largely due to our kick correction for field index deviation from m=1. Theoretically this correction should become perfect in the limit of zero length element slicing. Our numerical results are consistent with this.

SPIN COHERENCE TIME ESTIMATE

In estimating spin decoherence we need to account for the potential energy variation accompanying transverse position oscillations. Though the electric field is centrally directed within individual deflection elements, the centers of curvature of adjacent deflecting elements do not coincide. (Angular momentum components can be consistently propagated across drifts however.) Here, for simplicity, we restrict the discussion to a uniform, weak focusing lattice with no drift regions. We have to consider both "coasting beams" and the "bunched beams" that result with RF cavities in the ring.

Table 1: Comparisons of lattice functions calculated by linearized transfer matrix formalism and the arbitrary-amplitude UAL/ETEAPOT formalism, for the field index $m = 0$ cylindrical electrode case. (Vertical stability is provided by the very weak quadrupoles shown.)

file name	unit	linearized	"exact"
cells/arc		20	
bend radius	m	40.0	
half drift length	m	1.0	
half bend per cell	r	0.078539816	
half bend length	m	3.141592	
circumference	m	331.327	
quadrupole inverse focal length	1/m	-0.00005960	
field index		1.0e-10	
horizontal beta	m	36.1018	36.0962
vertical beta	m	263.6201	263.0767
horizontal tune		1.4578	1.4579
vertical tune		0.2000	0.2005

Figure 6 shows the spin vector **s** in relation to the design orbit. The evolution of the spin precession angle α, relative

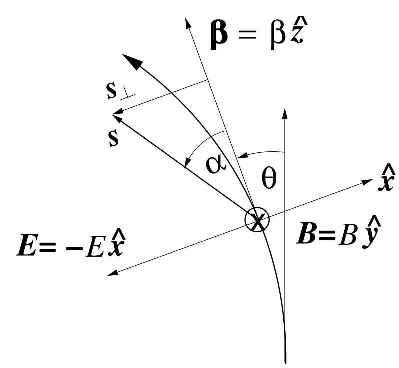

Figure 6: Spin vector **s** has precessed through angle α away from its nominal direction along the proton's velocity.

to the proton direction, is given by[11]

$$\frac{d\alpha}{dt} = \frac{eE(x)}{m_p c}\left(\frac{g\beta(x)}{2} - \frac{1}{\beta(x)}\right), \qquad (10)$$

where $g = 5.5857$ is the proton g-factor. The angular velocity in bend regions depends on the angular momentum L and radial coordinate r;

$$\frac{d\theta}{dt} = \frac{L}{\gamma m_p r^2}. \qquad (11)$$

L is a constant of the motion (because the force is radial) but γ and $r = r_0 + x$ depend on x. Eqs. (10) and (11) combine to give

$$\frac{d\alpha}{d\theta} = \frac{eE(x)(r_0+x)^2}{Lc\beta(x)}\left(\left(\frac{g}{2}-1\right)\gamma(x) - \frac{g/2}{\gamma(x)}\right), \qquad (12)$$

To find the evolution of α over long times we need to average this equation. Complicating this averaging is the fact that the final factor has been intentionally arranged to cancel for the central, design particle. The initial factor, though not constant, varies only over a small range, which tends to suppress correlations between the two factors. A promising approximation scheme is, therefore, to average the factors individually;

$$\left\langle\frac{d\alpha}{d\theta}\right\rangle = \left\langle\frac{eE(x)(r_0+x)^2}{Lc\beta(x)}\right\rangle\left(\left(\frac{g}{2}-1\right)\langle\gamma\rangle - \frac{g}{2}\left\langle\frac{1}{\gamma}\right\rangle\right). \tag{13}$$

The second factor depends only on γ (which varies along the orbit). For bunched beam operation this factorization is convenient, since γ deviates sinusoidally in storage ring operation at constant energy and is stabilized to average to the magic value γ_0. Only odd harmonics appear at large amplitudes, and they also cancel on the average. But the $1/\gamma$ factor in Eq. (13) does not average to $1/\gamma_0$.

The angle and time independent variables θ and t are very nearly, but not exactly proportional to each other. For coasting beams averages over θ and t are therefore not equivalent. But for bunched beams θ and t are strictly proportional (on the average) over long times, and the two forms of averaging should be equivalent.

The virial theorem can be used to obtain average behavior of multiparticle systems subject to central forces. We need to use a relativistic version of the theorem. “Virial” G is defined in terms of radius vector $\mathbf{r}$ and momentum $\mathbf{p}$ by

$$G = \mathbf{r}\cdot\mathbf{p}. \tag{14}$$

Our electric field is given by Eq. (1) and Newton’s law is given by Eq. (3). In a bending element the time rate of change of $\mathbf{G}$ is given by

$$\left.\frac{dG}{dt}\right|_{\rm bend} = m_pc^2\gamma - m_pc^2\,\frac{1}{\gamma} - eE_0r_0\,\frac{r_0^m}{r^m}. \tag{15}$$

Averaging over time, presuming bounded motion, and therefore requiring $\langle dG/dt\rangle$ to vanish, one obtains

$$\left\langle\frac{1}{\gamma}\right\rangle = \langle\gamma\rangle - \frac{E_0r_0}{m_pc^2/e}\left\langle\frac{r_0^m}{r^m}\right\rangle. \tag{16}$$

Applying this result, and $r = r_0 + x$, to average Eq. (13) yields

$$-\left\langle\frac{d\alpha}{d\theta}\right\rangle \approx \tag{17}$$
$$\frac{E_0r_0\gamma_0}{(p_0c/e)\beta_0}\left(\left\langle\frac{\gamma}{\gamma_0}-1\right\rangle + m\left\langle\frac{x}{r_0}\right\rangle - \frac{m^2-m}{2}\left\langle\frac{x^2}{r_0^2}\right\rangle\right).$$

Higher order terms in the expansion parameter $x/r_0 \approx 2\times10^{-4}$ have been dropped. Polarimeter/RF feedback forces the first term (in parenthesis) to cancel exactly. The factor $\langle x\rangle$ also tends to cancel over many betatron cycles. But changes of electric potential cause this cancellation to be imperfect. This term has a further factor of m. For the “cylindrical” case $m = 0$, suggesting that the optimal electrode shape will be at least approximately cylindrical. We also know, however, that $m = 0$ is singular, as regards the functioning of the lattice as a storage ring. (For $m = 0$ all circular orbits centered on the bend center have the same momentum, independent of radius.) We nevertheless anticipate designing the field index to be close to $m = 0$, consistent with the achievable energy acceptance.

If the parenthesized factor in Eq. (17) has a value of order 1, the spin coherence time would be measured in milliseconds, far too short for the EDM measurement to be feasible. But, taking $m = 1$ as a possible field index value, it can be seen that the parenthesized factor reduces to $\langle x/r_0\rangle$. Already of order 10^{-4}, this factor further averages to zero for linear betatron and synchrotron oscillations. It is hoped that careful lattice design, especially linearizing chromatic dependencies, along with small beam emittances, will produce adequately great SCT.

A major defect of this treatment has been that spin decoherence occurring on entrance to and exit from bend elements has been neglected. The same chromatic linearization is expected to reduce this decoherence mechanism to an acceptable level.

REFERENCES

[1] J. R. Ellis, M. K. Gaillard, D. V. Nanopoulos, and S. Rudaz, *A Cosmological Lower Bound on the Neutron Electric Dipole Moment,* Phys.Lett. B99 (1981) 101, 1981

[2] S. Weinberg, *Conference Summary (HEP Dallas conference 1992,* AIP Conf.Proc. 272, 346366, arXiv:hep-ph/9211298 [hep-ph], 1993

[3] Storage Ring EDM Collaboration, *A Proposal to Measure the Proton Electric Dipole Moment with 10^{-29} e-cm Sensitivity,* October, 2011

[4] Arkani-Hamed, *Pushing Beyond the LHC,*, Fundamental Physics at the Intensity Frontier Conference, Rockville MD, 2011

[5] N. Malitsky and R. Talman, *Unified Accelerator Libraries,* Proceedings of Conference on Accelerator Software, Williamsburg, VA, 1996, *The Framework of Unified Accelerator Libraries,* ICAP98, Monterey, 1998

[6] L. Schachinger and R. Talman, *TEAPOT: A Thin Element Program for Optics and Tracking,* Part. Accel. **22**,35, 1987

[7] G. Muñoz and I. Pavic, *A Hamilton-like vector for the special-relativistic Coulomb problem,* Eur. J. Phys. **27**, 1007-1018, 2006

[8] C. Møller, *The Theory of Relativity,* Clarendon Press, Oxford, 1952

[9] T. Boyer, Am. J. Phys. **72** (8) 992, 2004

[10] H. Wollnik, *Optics of Charged Particles,* Academic Press, p. 124, 1987

[11] J. Jackson, *Classical Electrodynamics,* 3rd edition, John Wiley, 1998

ISBN 978-3-95450-115-1